

# Deep Learning-based Codes for Wiretap Fading Channels

Daniel Seifert\*, Onur Günlü†, and Rafael F. Schaefer\*

\*Chair of Information Theory and Machine Learning, Dresden University of Technology (TU Dresden), Germany

†Information Theory and Security Laboratory (ITSL), Linköping University, Sweden

{daniel.seifert, rafael.schaefer}@tu-dresden.de, onur.gunlu@liu.se

**Abstract**—The wiretap channel is a well-studied problem in the physical layer security (PLS) literature. Although it is proven that the decoding error probability and information leakage can be made arbitrarily small in the asymptotic regime, further research on finite-blocklength codes is required on the path towards practical, secure communications systems. This work provides the first experimental characterization of a deep learning-based, finite-blocklength modular code construction for multi-tap fading wiretap channels without channel state information (CSI). In addition to the evaluation of the average probability of error and information leakage, we illustrate the influence of (i) the number of fading taps, (ii) differing variances of the fading coefficients and (iii) the seed selection for the hash function-based security layer.

**Index Terms**—Physical layer security, wiretap channel, autoencoder, deep learning, machine learning for communications.

## I. INTRODUCTION

Physical layer security (PLS) is a promising field of research that aims to guarantee security in communications systems by directly integrating it into the physical layer. In contrast to conventional means of security that fully rely on computational constraints of the adversary, PLS focuses solely on information-theoretic measures to describe provable notions of security [1].

A fundamental model in PLS is the wiretap channel where the sender (Alice) wants to transmit a confidential message  $M \in \{0, 1\}^k$  to the legitimate receiver (Bob). This message is encoded as a block  $X^n \in \mathcal{X}^n$  of length  $n$ , sent over the channel and received by Bob as  $Y^n \in \mathcal{Y}^n$ . However, a malicious eavesdropper (Eve) is able to learn information about this message via her channel observations  $Z^n \in \mathcal{Z}^n$ . [2] and [3] showed that the average probability of decoding error and the information leakage can be made arbitrarily small for infinitely long codewords, using a random-coding argument. Moreover, conventional channel codes, such as low-density parity check (LDPC) [4] and polar codes [5], have been adopted to construct secrecy capacity-achieving wiretap channel codes (WTC). In practical systems that require low-latency and hence, short packets, the assumption of infinite

This work was supported in part by the Federal Ministry of Education and Research of Germany (BMBF) within the project 6G-life, Project ID 16KISK001K, by the ZENITH Research and Leadership Career Development Fund, Chalmers Transport Area of Advance, and the ELLIIT funding endowed by the Swedish government. Moreover, it was supported by the Cluster of Excellence “Centre for Tactile Internet with Human-in-the-Loop” (CeTI) of Technische Universität Dresden of the German Research Foundation (DFG) EXC 2050/1, Projekt ID 390696704.

blocklength is not valid anymore. Accordingly, [6] derived achievability and converse bounds on the secrecy capacity in the non-asymptotic regime.

Modular coding schemes for the wiretap channel, composed of an error-correcting code and a security component were first proposed by [7], bridging the gap between information-theoretic and cryptographic security. [8] and [9] applied this modular approach, by deploying universal hash functions (UHF) as the security component, in the context of semantic security. Furthermore, [10] proposed the usage of deep learning-based channel codes as the reliability module in combination with an UHF and evaluated the performance of these codes for Gaussian wiretap channels. However, research on finite-blocklength wiretap codes for fading channels is still scarce. Recently, [11] provided a secrecy performance study for finite-blocklength transmissions in fading channels with instantaneous channel state information (CSI) of Bob’s channel available at the transmitter.

In this work, we evaluate the seeded modular wiretap code design approach from [10] on more complex channel models, namely multi-tap Rayleigh fading, and assume complete absence of CSI. We evaluate the average probability of error and information leakage performance for both varying and constant communication rate scenarios. Moreover, we illustrate the benefits from more channel taps as well as stochastical degradedness in terms of the information leakage. Finally, in contrast to schemes based on classical channel codes, we find that the selection of seeds to the UHF does not have an influence on the Hamming and Lee distances and, therefore, on the information leakage of the overall system.

## II. SYSTEM MODEL

We consider a real-valued,  $T$ -tap fading wiretap channel  $(\mathcal{X}, p_{YZ|X}, \mathcal{Y} \times \mathcal{Z})$  given by

$$Y_i = \sum_{t=0}^{T-1} H_{Y,t} X_{i-t} + N_Y, \quad Z_i = \sum_{t=0}^{T-1} H_{Z,t} X_{i-t} + N_Z \quad (1)$$

where  $N_Y$  and  $N_Z$  denote the zero-mean Gaussian random variables with variances  $\sigma_Y^2 = (2R_r E_b / N_{0,Y})^{-1}$  and  $\sigma_Z^2 = (2R_r E_b / N_{0,Z})^{-1}$ . We define  $E_b / N_{0,Y}$  and  $E_b / N_{0,Z}$  as the per-bit energy to noise power spectral density ratio on Bob’s and Eve’s channel, respectively, and  $R_r$  as the encoding rate of the reliability layer (see Section II-A1). Due to this

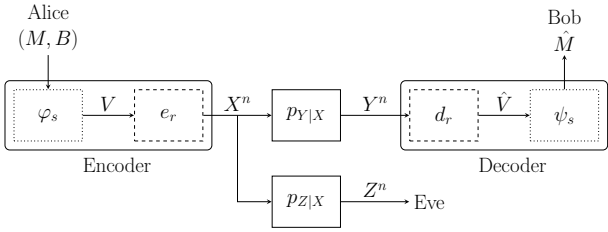


Fig. 1: Modular wiretap code design comprised of the reliability layer ( $e_r, d_r$ ) and the security layer ( $\varphi_s, \psi_s$ ).

scaling we allow for a fair comparison of codes with different rates.  $H_{Y,t}$  and  $H_{Z,t}$  denote the magnitudes of the  $t$ -th tap fading coefficients, that follow Rayleigh distributions such that  $H_Y \sim \mathcal{CN}(0, \sigma_{H_Y}^2 T^{-1})$  and  $H_Z \sim \mathcal{CN}(0, \sigma_{H_Z}^2 T^{-1})$ , which are normalized with respect to the number of fading taps to meet the unit power constraint. Note that selecting  $T > 1$  results in intersymbol interference (ISI).

*Definition 1* ([12]): The fading wiretap channel in (1) is stochastically degraded if  $H_Y/\sigma_Y^2$  is stochastically larger than  $H_Z/\sigma_Z^2$ , i.e., for all  $h \geq 0$ , we have

$$\bar{F}_{H_Y}(h/\sigma_Y^2) \geq \bar{F}_{H_Z}(h/\sigma_Z^2) \quad (2)$$

where  $\bar{F}_X(x) = \Pr(X \geq x)$  is the complementary cumulative distribution function of a real-valued random variable  $X$ .

#### A. Wiretap Code

Codes for the wiretap channel aim to provide a certain level of security in a scenario where the confidential communication over the channel is eavesdropped by another user. In order to quantify their performance, one resorts to the following metrics:

- We measure the *reliability* of the system in terms of the average probability of error at the legitimate receiver Bob, i.e.,  $P_e \triangleq \Pr(\hat{M} \neq M)$  where  $\hat{M}$  denotes the decoded message. Practically, it will be estimated by the block error rate (BLER), averaged over a run of Monte Carlo simulations.
- The *secrecy* is determined by the amount of information about the source message  $M$  that is leaked to Eve via her channel observations  $Z^n$ . This leakage is denoted as  $L \triangleq I(M; Z^n)$ .

*Definition 2* ([10]): An  $(n, k, P)$  code is  $\epsilon$ -reliable if  $P_e \leq \epsilon$  and  $\delta$ -secure if  $L \leq \delta$ . Moreover, a secure communication rate  $R_s = k/n$  is  $(\epsilon, \delta)$ -achievable with power constraint  $P$  if there exists an  $\epsilon$ -reliable and  $\delta$ -secure  $(n, k, P)$  code.

We consider the modular coding scheme proposed in [10], depicted in Fig. 1. This scheme guarantees the reliability and security constraints by an implementation consisting of two separately designed layers. A key advantage of this separation-based approach is its flexibility with respect to the redesign of any of these layers. In the following, we will briefly discuss the details of each layer.

1) *Reliability Layer*: The encoder-decoder pair  $(e_r, d_r)$  of the reliability layer is implemented by an artificial neural network. Using an autoencoder structure [13], the encoder

TABLE I: Configuration of the autoencoder network.

	Layers	Input Size	Output Size
Encoder	One-hot Encoder	$q$	$Q$
	FC Layer + ReLU	$Q$	$n$
	FC Layer + Linear	$n$	$n$
	Normalization	$n$	$n$
Decoder	FC Layer + ReLU	$n$	$n$
	FC Layer + Softmax	$n$	$Q$

and decoder parts are jointly optimized to minimize the BLER. Similar to classical channel codes, the encoder adds redundancy by learning new representations of the source messages in order to make it more robust to perturbations caused by the channel, while the decoder aims to recover the original message by exploiting the redundancy. Table I shows the configuration of the autoencoder that is composed of a sequence of fully-connected (FC) layers with either rectified linear units (ReLU) or linear activation functions. It is trained using stochastic gradient decent (SGD) with the categorical cross-entropy loss function between the one-hot encoded message as ground truth and the softmax output of the decoder. This loss function inherently optimizes for the BLER [14]. The encoding rate of the reliability layer is then  $R_r = q/n$ .

2) *Security Layer*: The security layer aims to control the amount of information about the source message  $M$  that is leaked to Eve via her channel observations  $Z^n$ . This can be achieved by the use of a 2-UHF  $\psi_s$  and its inverse  $\varphi_s$ , as defined below. Both of these functions rely on a seed  $s \in \mathcal{S} = \{0, 1\}^q \setminus \{\mathbf{0}\}$  that is assumed to be known by all parties. In addition, for every message  $M$  Alice samples a uniformly distributed random bit sequence  $B \in \{0, 1\}^{q-k}$  as a means of randomization to the output of  $\varphi_s$ .

*Definition 3* ([15]): Let  $\mathcal{A}$  and  $\mathcal{B}$  be finite sets and  $\mathcal{F}$  a subset of the set of all mappings  $\mathcal{A} \rightarrow \mathcal{B}$ , then  $\mathcal{F}$  is a family of 2-universal hash functions (2-UHF) if  $\Pr(F(x) = F(y)) \leq |\mathcal{B}|^{-1}$  where  $x, y \in \mathcal{A}$  and  $F$  is uniformly drawn from  $\mathcal{F}$ .

On the encoder side, we define the inverse function as

$$\varphi_s : \{0, 1\}^k \times \{0, 1\}^{q-k} \rightarrow \{0, 1\}^q \quad (3)$$

$$(m, b) \mapsto s^{-1} \odot (m||b) \quad (4)$$

where  $\odot$  denotes the multiplication in  $\text{GF}(2^q)$  and  $(\cdot||\cdot)$  the concatenation of two bit sequences. After passing the reliability layer  $d_r$  within the decoder, the source message  $M$  is recovered by applying the hash function

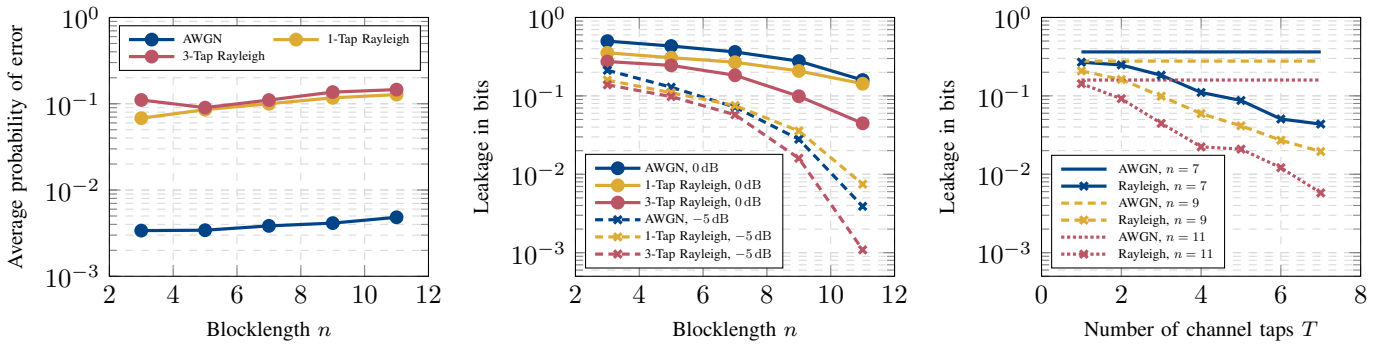
$$\psi_s : \{0, 1\}^q \rightarrow \{0, 1\}^k \quad (5)$$

$$v \mapsto (s \odot v)_k \quad (6)$$

where  $(\cdot)_k$  denotes the truncation of the bit sequence to the  $k$  most significant bits.

#### B. Mutual Information Estimation

We want to estimate the information leakage by the mutual information  $I(M; Z^n)$ . As the analytical expressions for the respective joint and marginal probability distributions are



(a) Average error probability at Bob over blocklength  $n$  for  $E_b/N_{0,Y} = 5$  dB.

(b) Information leakage to Eve over blocklength  $n$  for varying  $E_b/N_{0,Z}$ .

(c) Information leakage to Eve over number of fading channel taps  $T$  for  $E_b/N_{0,Z} = 0$  dB.

Fig. 2: Reliability and security evaluation of the designed WTC for variable rates  $R_s = 1/n$ ,  $R_r = (n-1)/n$ ,  $E_b/N_{0,Y} > E_b/N_{0,Z}$  and  $\sigma_{H_Y}^2 = \sigma_{H_Z}^2$ .

unknown, we resort to a sample-based estimation approach. This can practically be accomplished by deploying the *Mutual Information Neural Estimator* (MINE) [16] that is based on a variational representation of the Kullback-Leibler (KL) divergence and provides a lower bound on the mutual information. We can parameterize a function  $T_\theta$ , represented by a neural network, to obtain an estimate

$$\hat{I}(M; Z^n) \hat{=} \sup_{\theta \in \Theta} \left[ \frac{1}{N} \sum_{i=1}^N T_\theta(m(i), z^n(i)) - \log \left( \frac{1}{N} \sum_{i=1}^N \exp^{T_\theta(\tilde{m}(i), \tilde{z}^n(i))} \right) \right] \quad (7)$$

where  $N$  input samples  $(m(i), z^n(i))$  are drawn from  $p_{MZ^n}$  and  $(\tilde{m}(i), \tilde{z}^n(i))$  from  $p_{MPZ^n}$ , respectively. Throughout this work, the parameterized neural network of MINE is implemented by a sequence of four FC layers with 400 neurons and ReLU activation each, except for the last layer that is followed by a linear activation. Training is performed using SGD with an exponentially decaying learning rate to ensure a smooth convergence.

### III. MAIN RESULTS

#### A. Variable Rates

For the first characterization of the constructed WTC, we examine the previously defined reliability and security metrics. As in [10], we will consider  $k = 1$  and  $q = n - 1$  such that  $R_s = 1/n$  and  $R_r = (n-1)/n$ . Since MINE suffers from an increased bias and variance for high-dimensional probability distributions [17], we focus on short blocklengths. Moreover,  $E_b/N_{0,Y} = 5$  dB is kept fixed for all simulations, while  $E_b/N_{0,Z} = \{-5, 0\}$  dB is selected to investigate the scenario when Bob's advantage with respect to noise level declines. We fix the distribution of fading coefficients for both channels by choosing  $\sigma_{H_Y}^2 = \sigma_{H_Z}^2$ .

From Fig. 2a it can be observed that the multi-tap fading channel poses a greater challenge to the decoder and, therefore, introduces more errors. In contrast, Fig. 2b shows that fading can be beneficial for secure communication as it significantly lowers the leakage to the eavesdropper. Similar to the AWGN

case, the information leakage decreases with higher blocklengths. However, when decreasing  $E_b/N_{0,Z}$ , the intersection point of the AWGN and the single-tap fading scenarios moves towards smaller blocklengths.

Moreover, we assess the leakage to Eve with an increasing number of channel taps, i.e. a higher amount of ISI within one block, illustrated in Fig. 2c. While for  $L = 1$  there is only a slight reduction in leakage with respect to the AWGN case, the leakage is significantly lowered for channels with an increased number of fading taps.

#### B. Constant Rates

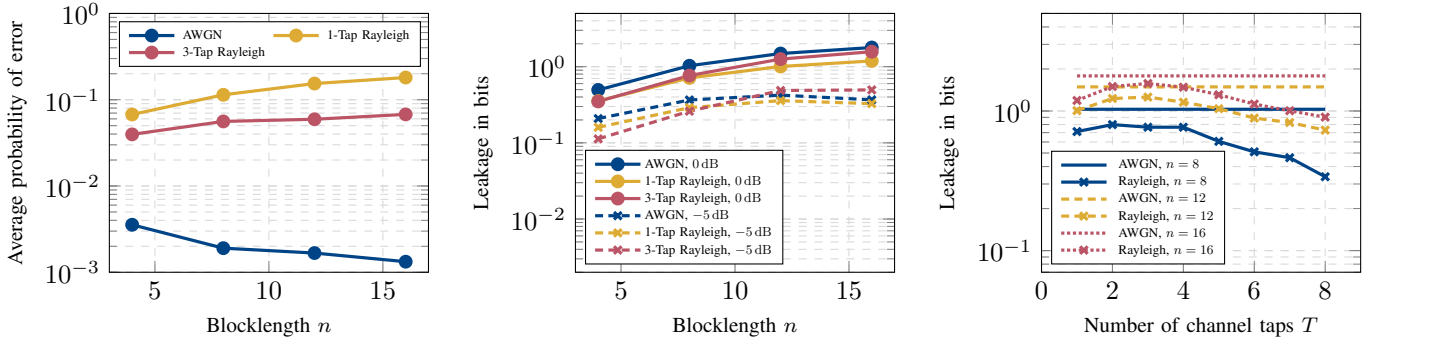
In order to provide a fair comparison among codes of different blocklengths, we keep the rates constant as  $R_s = 1/4$  and  $R_r = 1/2$ , and evaluate the experiments from Section III-A for the same configuration for both channels.

Fig. 3a depicts the average probability of error at Bob over varying blocklengths. In contrast to the gap between AWGN and the Rayleigh fading scenarios that were observed in the previous experiment, the 3-tap channel outperforms the single-tap one. It seems that the learned decoder at Bob takes advantage of the symbol correlations caused by ISI. We observed the same pattern in our experiments with a comparable rate (7, 4)-Hamming code with maximum-likelihood sequence estimation.

Furthermore, the leakage to Eve over varying blocklengths is displayed in Fig. 3b for two different noise levels. At  $E_b/N_{0,Z} = 0$  dB the leakage for the fading channels is generally lower than for the AWGN channel. However, while the single-tap fading case maintains a constant gap to the AWGN case, the leakage for the 3-tap fading channel closes this gap for higher blocklengths. A similar observation is made at  $E_b/N_{0,Z} = -5$  dB, where the leakage of the 3-tap channel even surpasses the AWGN case. Consequently, the effect of leakage reduction with an increase of fading channel taps is also present in the constant rate setup, as shown in Fig. 3c.

#### C. Fading Coefficient Variance Analysis

Next, we consider the scenario of Eve's channel being stochastically degraded with respect to Bob's only via the variances  $\sigma_{H_Y}^2$  and  $\sigma_{H_Z}^2$ , which define the Rayleigh distribution of



(a) Average error probability at Bob over blocklength  $n$  for  $E_b/N_0,Y = 5$  dB.  
(b) Information leakage to Eve over blocklength  $n$  for varying  $E_b/N_0,Z$ .  
(c) Information leakage to Eve over number of fading channel taps  $T$  for  $E_b/N_0,Z = 0$  dB.

Fig. 3: Reliability and security evaluation of the designed WTC for constant rates  $R_s = 1/4$ ,  $R_r = 1/2$ ,  $E_b/N_0,Y > E_b/N_0,Z$  and  $\sigma_{H_Y}^2 = \sigma_{H_Z}^2$ .

the fading coefficients, whereas the noise levels of both channels stay the same, i.e.  $\sigma_Y^2 = \sigma_Z^2$ . In this case, the condition (2) is fulfilled if  $d = \sigma_{H_Y}^2/\sigma_{H_Z}^2 \geq 1$ . In the following, we will express the changes in the variance of the fading coefficients of Eve's channel via  $d$ . The communication rates  $R_s$  and  $R_r$  are chosen as in Section III-A. From Fig. 4 it can be observed that increasing  $d$ , i.e., lowering  $\sigma_{H_Z}^2$ , significantly reduces the leakage. This is expected, since a Rayleigh distribution with a more narrow spread and its peak closer to zero ultimately results in a higher number of lower-magnitude realizations, attenuating Eve's channel observations  $Z^n$ .

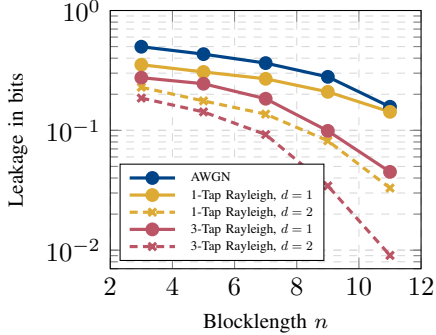


Fig. 4: Information leakage to Eve over blocklength  $n$  for varying factors  $d = \sigma_{H_Y}^2/\sigma_{H_Z}^2$  and  $E_b/N_0,Y = E_b/N_0,Z = 0$  dB.

#### D. Seed Selection

Up to this point, we assumed the same fixed set of seeds  $s$  as in [10]. The authors of [18] examined a modular wiretap code design involving a polar code-based reliability layer and a similar UHF-based security layer with respect to Eve's advantage, using distinguishing security as the security metric. They found the seed selection to be crucial to this metric and classified the seeds with respect to the dispersion of the distribution of the average Hamming distance  $d_H$  between two encoded messages  $m_1$  and  $m_2$  using the same seed  $s$ . As our reliability layer  $e_r$  comprises both channel coding and modulation, we will apply an  $l$ -level quantization stage to the real-valued output of the encoder to enable a similar examination. The quantized encoder output is denoted by  $\bar{e}_r$ . In addition to the Hamming distance, we will consider the Lee distance  $d_L$  over the  $l$ -ary alphabet [19] since it provides a more nuanced distance evaluation for non-binary words.

For the configuration  $k = 4$ ,  $q = 8$ , and  $n = 16$ , we calculated the distances  $d_H((\bar{e}_r(\varphi_s(m_1, b)), \bar{e}_r(\varphi_s(m_2, b)))$  and  $d_L(\bar{e}_r(\varphi_s(m_1, b)), \bar{e}_r(\varphi_s(m_2, b)))$  for each seed  $s$ , including all possible combinations of messages  $m_1$  and  $m_2$  with  $m_1 \neq m_2$  and random bits  $b$ . The selected quantizer has a step size of  $l = 16$ . As an example, Fig. 5 depicts the empirical distribution for both distance metrics for  $s = (0, 0, 0, 0, 0, 0, 1, 1)$ . In contrast to the findings of [18], it was observed that these statistics remain the same for all possible seeds, i.e., the selection of seeds does not have a significant influence on the output of the designed WTC. Moreover, we verified this observation by the information leakage analysis that does not show major deviations when choosing different seeds.

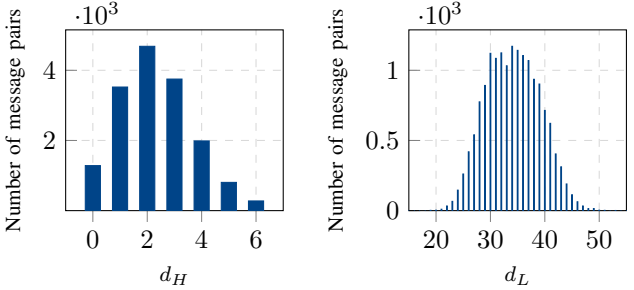


Fig. 5: Histograms of Hamming distances  $d_H$  and Lee distances  $d_L$  for the 16-step quantized encoder output for all possible combinations of message pairs  $(m_1, m_2)$  with  $m_1 \neq m_2$  and random bits  $b$ , for the WTC with  $k = 4$ ,  $q = 8$  and  $n = 16$  and  $s = (0, 0, 0, 0, 0, 0, 1, 1)$ .

#### IV. CONCLUSION

We adopted a framework for a modular wiretap code design consisting of a learned channel code as reliability layer and a UHF as security layer for multi-tap fading channels without CSI, and experimentally assessed its performance. In comparison to the AWGN case, we observe a performance loss in terms of reliability. However, fading can help to significantly decrease the information leakage. Moreover, the increase of fading taps as well as a lower variance of the fading coefficients of Eve's channel can further diminish the information leakage. Finally, we found, in contrast to modular wiretap codes designs that involve classical codes, that the choice of seeds does not make a significant difference for our autoencoder-based setup. Future work will focus on extensions towards larger, more practical blocklengths.

## REFERENCES

- [1] M. Bloch and J. Barros, *Physical-Layer Security: From Information Theory to Security Engineering*. Cambridge University Press, 2011.
- [2] A. D. Wyner, “The wire-tap channel,” *The Bell System Technical Journal*, vol. 54, no. 8, pp. 1355–1387, Oct. 1975.
- [3] I. Csiszár and J. Körner, “Broadcast channels with confidential messages,” *IEEE Trans. Inf. Theory*, vol. 24, no. 3, pp. 339–348, May 1978.
- [4] A. Thangaraj *et al.*, “Applications of ldpc codes to the wiretap channel,” *IEEE Trans. Inf. Theory*, vol. 53, no. 8, pp. 2933–2945, Aug. 2007.
- [5] H. Mahdavifar and A. Vardy, “Achieving the secrecy capacity of wiretap channels using polar codes,” *IEEE Trans. Inf. Theory*, vol. 57, no. 10, pp. 6428–6443, Oct. 2011.
- [6] W. Yang, R. F. Schaefer, and H. V. Poor, “Wiretap channels: Nonasymptotic fundamental limits,” *IEEE Trans. Inf. Theory*, vol. 65, no. 7, pp. 4069–4093, July 2019.
- [7] M. Bellare, S. Tessaro, and A. Vardy, “A cryptographic treatment of the wiretap channel,” Jan. 2012, arXiv:1201.2205 [Online].
- [8] M. Wiese and H. Boche, “Semantic security via seeded modular coding schemes and ramanujan graphs,” *IEEE Trans. Inf. Theory*, vol. 67, no. 1, pp. 52–80, Jan. 2021.
- [9] L. Torres-Figueredo *et al.*, “Experimental evaluation of a modular coding scheme for physical layer security,” in *IEEE Global Communications Conference*, Dec. 2021, pp. 1–6.
- [10] V. Rana and R. A. Chou, “Short blocklength wiretap channel codes via deep learning: Design and performance evaluation,” *IEEE Trans. Commun.*, vol. 71, no. 3, pp. 1462–1474, Mar. 2023.
- [11] M. T. Mamaghani *et al.*, “Performance analysis of finite blocklength transmissions over wiretap fading channels: An average information leakage perspective,” *IEEE Trans. Wireless Commun.*, pp. 1–1, May 2024.
- [12] M. Mittelbach *et al.*, “Secure integrated sensing and communication under correlated rayleigh fading,” Aug. 2024, arXiv:2408.17050 [Online].
- [13] T. O’Shea and J. Hoydis, “An introduction to deep learning for the physical layer,” *IEEE Trans. on Cogn. Commun. Netw.*, vol. 3, no. 4, pp. 563–575, Oct. 2017.
- [14] R. Wiesmayr, G. Marti, C. Dick, H. Song, and C. Studer, “Bit error and block error rate training for ML-assisted communication,” in *IEEE International Conference on Acoustics, Speech and Signal Processing*, June 2023, pp. 1–5.
- [15] Hayashi, M. and Matsumoto, R., “Construction of wiretap codes from ordinary channel codes,” in *IEEE International Symposium on Information Theory*, June 2010, pp. 2538–2542.
- [16] M. I. Belghazi *et al.*, “Mutual information neural estimation,” in *International Conference on Machine Learning*, vol. 80, July 2018, pp. 531–540.
- [17] J. Song and S. Ermon, “Understanding the limitations of variational mutual information estimators,” in *International Conference on Learning Representations*, Apr. 2020.
- [18] A. Frank *et al.*, “Implementation of a modular coding scheme for secure communication,” in *IEEE International Conference on Communications*, May 2022, pp. 2900–2905.
- [19] C. Lee, “Some properties of nonbinary error-correcting codes,” *IRE Trans. Inf. Theory*, vol. 4, no. 2, pp. 77–82, June 1958.